Millimeter-Wavelength Cloud Measurements Taken with the Polarimetric Cloud Profiling Radar System

S. M. Sekelsky and R. E. McIntosh
Microwave Remote Sensing Laboratory
University of Massachusetts
Amherst, Massachusetts

Introduction

This paper reviews hardware for the Cloud Profiling Radar System (CPRS) and presents dual-frequency measurements that illustrate how CPRS reflectivity data may be used for cloud particle sizing. Reflectivity data show Mie scattering in the ice region, melting layer, and rain region of a stratiform cloud with light, broken precipitation. Measurements of Ze_{95} and Ze_{33} with and without precipitation show that differential attenuation is low and does not dominate the reflectivity differences. A theoretical model of Ze_{95} - Ze_{33} versus mean particle diameter for monodisperse and Gaussian size distributions of water droplets is presented to illustrate the concept of particle sizing using dual-wavelength reflectivity data.

Hardware for the Cloud Profiling Radar System

The CPRS is a versatile, high-resolution, mobile radar. The radar and supporting hardware are mounted on a half-flatbed/half-cube truck that serves as a self-contained mobile laboratory. The truck carries all the radar equipment and is thus an economical means of transport. The radar and low cross-polarization lens antenna sit atop an elevation-over-azimuth pedestal on the flatbed portion of the truck. The programmable pedestal facilitates high-resolution, 3-D scanning. Hydraulic jacks under the truck body level the truck and stabilize it against the wind. A 14'-long cube section houses equipment racks and work areas for the radar operator and technician. The truck has an on-board 10-kW electrical generator that provides power for the radar and the built-in heater/air conditioner and lights. The 100-gallon fuel tank allows the radar to operate continuously for over a week before refueling.

The radar consists of 33-GHz and 95-GHz subsystems, which transmit and receive through a single, 1-meter diameter dielectric lens antenna. The single aperture eliminates antenna pointing errors which are especially significant here where the 33-GHz and 95-GHz beamwidths are 0.5 degrees and 0.18 degrees, respectively. Each subsystem can transmit vertically or horizontally polarized pulses, where the transmit polarizations are selectable on a pulse-to-pulse basis. Each subsystem has a dual-channel receiver that coherently measures the vertical and horizontal components of the backscattered signal. System parameters are summarized in Table 1.

Table 1. Characteristics of 33-GHz and 95-GHz Radars

	Ka-band Radar	W-band Radar
Frequency	33.12 GHz	94.92 GHz
Peak Power	100 kW	1.5 kW
Average Power	120 W	15 W
PRF	200 Hz - 3 kHz (20 kHz bursts)	1 Hz - 80 kHz
Pulsewidth	200 - 2000 ns	50 - 2000 ns
Noise Figure	11 dB	13 dB
3 dB Bandwidth	5 MHz	5 MHz
3 dB Beamwidth	0.5 deg	0.18 deg

Cloud Measurements

Figures 1 and 2 are reflectivity images taken with the radar pointing toward zenith. Based on polarimetric and Doppler measurements, the melting layer height was estimated to be approximately 4.8 km. Therefore, the cloud above this

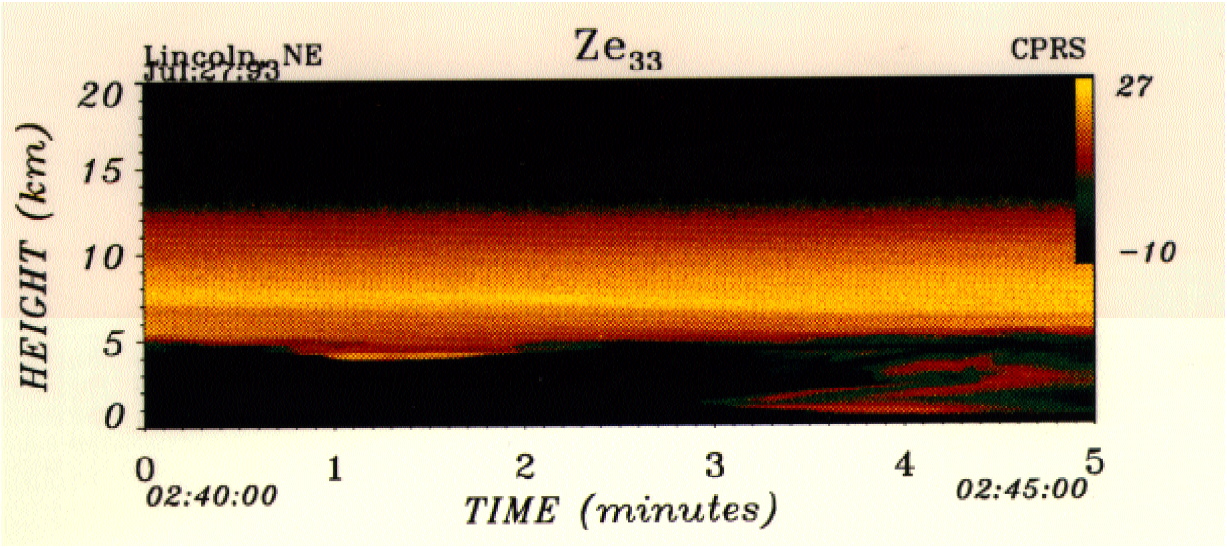

Figure 1. 33-GHz reflectivity image.

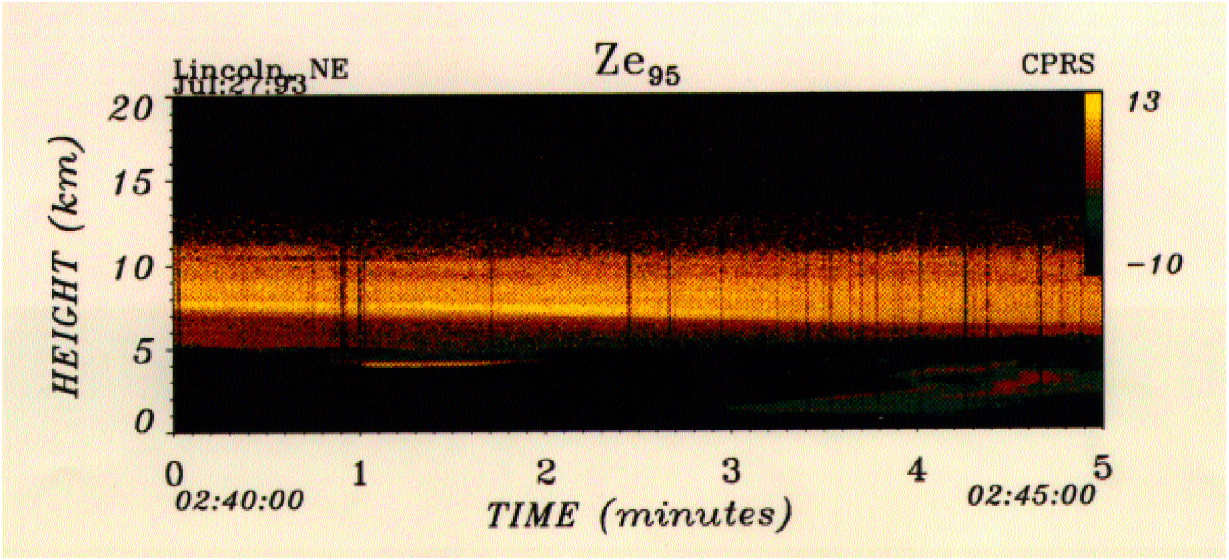

Figure 2. 95 GHz reflectivity image.

level is composed primarily of ice particles. The fact that the cloud shows a great deal of horizontal uniformity and that the peak values of cloud reflectivity are the same both before and during the rain suggests that differential attenuation through the rain is low.

Profiles of these images, shown in Figures 3 and 4, reveal substantial differences in 95-GHz and 33-GHz reflectivities in both the rain and in the ice cloud. The range of measured values of the difference for rain fall within the range predicted by the models plotted in Figure 5. Although the

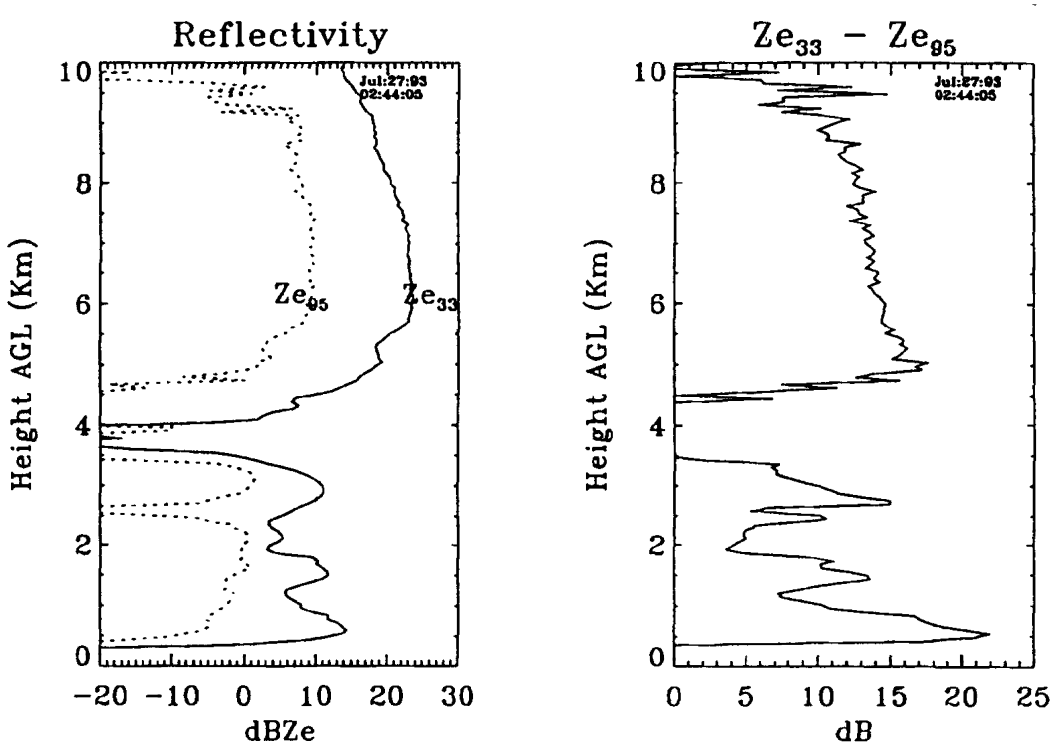

Figure 3. Reflectivity profile through rain.

true drop size distribution (DSD) of the rain was not measured, Figure 5 can be used to estimate mean drop size in rain, provided the true distribution is narrow. As the DSD width increases, the peaks in Figure 5 flatten, as is illustrated by the dashed curve for a Gaussian distribution. Measurements of larger particles also become more ambiguous for wider distributions. For instance, the peak value of Ze_{95} - Ze_{33} in Figure 3 suggests that the average particle diameter at 0.5 km may be 1.7 mm or 2.8 mm, depending on the width of the distribution. Doppler measurements may eliminate size ambiguities in Figure 5 and provide further insight into the shape of the DSD.

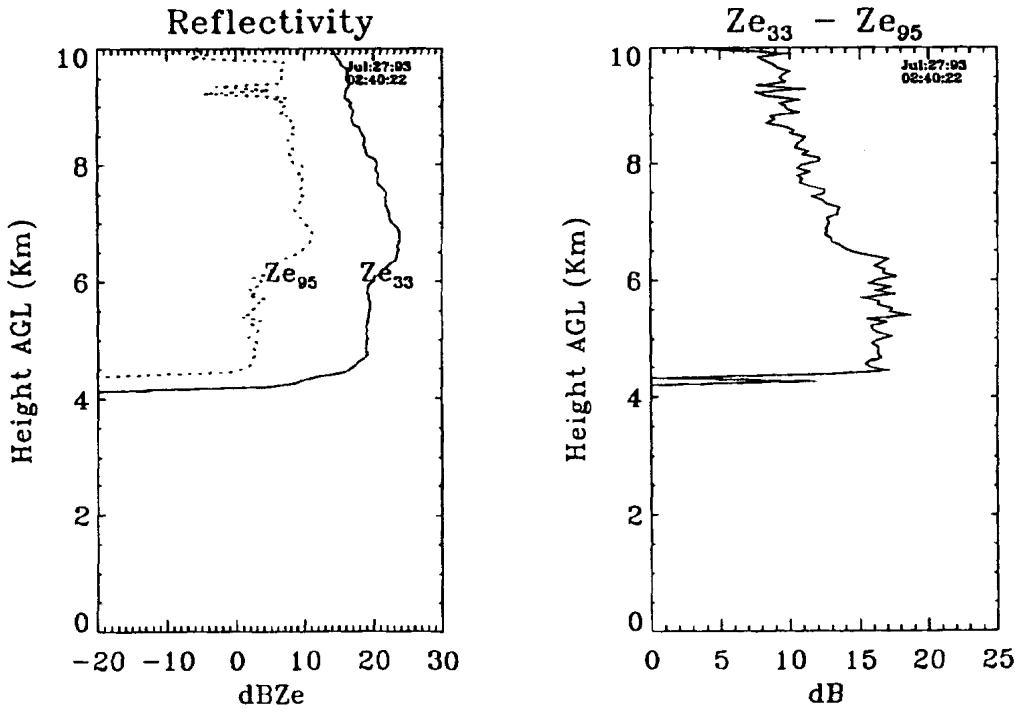

Figure 4. Reflectivity profile through rainfree region.

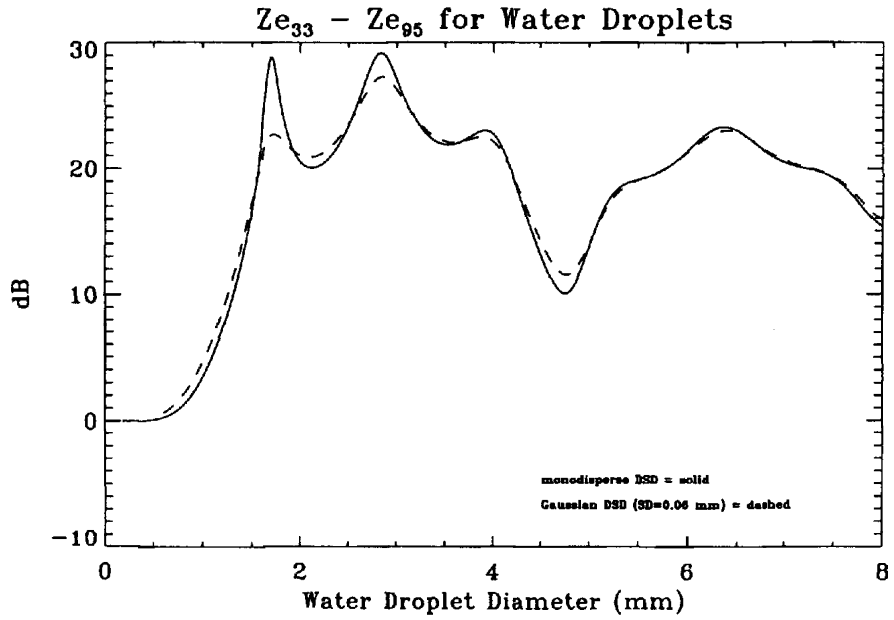

Figure 5. Theoretical Ze_{95} - Ze_{33} for monodisperse and Gaussian drop size distributions.